Biochimica et Biophysica Acta 1808 (2011) 1921–1929

Contents lists available at ScienceDirect

Biochimica et Biophysica Acta

journal homepage: www.elsevier.com/locate/bbamem

Reorganization of the actin cytoskeleton upon G-protein coupled receptor signaling

Sourav Ganguly, Roopali Saxena, Amitabha Chattopadhyay *

Centre for Cellular and Molecular Biology, Council of Scientific and Industrial Research, Uppal Road, Hyderabad 500 007, India

ARTICLE INFO

Article history:
Received 12 February 2011
Received in revised form 29 March 2011
Accepted 1 April 2011
Available online 9 April 2011

Keywords:
Actin
cAMP
Cytoskeleton
GPCR
Serotonin$_{1A}$ receptor

ABSTRACT

The actin cytoskeleton is involved in a multitude of cellular responses besides providing structural support. While the role of the actin cytoskeleton in cellular processes such as trafficking and motility has been extensively studied, reorganization of the actin cytoskeleton upon signaling by G-protein coupled receptors (GPCRs) represents a relatively unexplored area. The G-protein coupled receptor superfamily is an important protein family in mammals, involved in signal transduction across membranes. G-protein coupled receptors act as major signaling hubs and drug targets. The serotonin$_{1A}$ receptor is a representative member of the G-protein coupled receptor superfamily and plays a crucial role in the generation and modulation of various cognitive, developmental and behavioral functions. In order to monitor the changes in the actin cytoskeleton upon serotonin$_{1A}$ receptor signaling in a quantitative manner, we developed an approach based on high magnification imaging of F-actin in cells, followed by image reconstruction. Our results suggest that the actin cytoskeleton is reorganized in response to serotonin$_{1A}$ receptor signaling. In addition, we show that reorganization of the actin cytoskeleton is strongly dependent on adenosine 3′,5′-cyclic monophosphate level, and is mediated by the activation of protein kinase A. Our results are consistent with the possibility of a feedback mechanism involving the actin cytoskeleton, adenosine 3′,5′-cyclic monophosphate level and the serotonin$_{1A}$ receptor.

1. Introduction

G-protein coupled receptors (GPCRs) constitute the largest family of cell surface receptors and are involved in the transduction of extracellular stimulus to cellular interior [1,2]. These receptors are activated by a wide variety of ligands (stimuli) ranging from biogenic amines, amino acids, ions, peptides, proteins, and even photons [3]. GPCRs are prototypical members of the family of seven transmembrane domain proteins and include >800 members which together constitute ~5% of the human genome [4]. GPCRs mediate multiple physiological processes such as neurotransmission, cellular metabolism, secretion, cellular differentiation, growth, inflammatory and immune responses. It is therefore only natural that GPCRs have emerged as major targets for the development of novel drug candidates in all clinical areas and represent ~50% of current drug targets [5,6]. Interestingly, although GPCRs represent ~50% of current drug targets, only a small fraction of all GPCRs are presently targeted by drugs [7]. This points out the exciting possibility that the receptors that are not recognized yet could be potential drug targets for diseases that are difficult to treat by currently available drugs. In the overall context of the importance of GPCRs in cellular signaling and their potential as drug targets, GPCR biology represents an ever expanding, and keenly studied area of research in contemporary biology.

Cellular signaling by GPCRs involves their activation by ligands present in the extracellular environment and the subsequent transduction of signals to the interior of the cell through concerted changes in their transmembrane domain structure [8]. The major paradigm in GPCR signaling is that ligand mediated stimulation of these receptors leads to the activation of heterotrimeric GTP-binding proteins (G-proteins) [9]. The key steps involved in this process are agonist-induced guanine nucleotide exchange of GDP by GTP on the G-protein α subunit. This is followed by conformational changes in the GPCR and dissociation or rearrangement of the Gα from Gβγ subunits. The activated G-protein subunits subsequently elicit an array of downstream signaling events by interacting with specific effectors like adenylyl cyclases (AC), phospholipases or ion channels. Specifically, activation/deactivation of ACs further results in the up/downregulation of cyclic AMP (cAMP) level.

The serotonin$_{1A}$ (5-HT$_{1A}$) receptor is an important neurotransmitter receptor and belongs to the superfamily of the seven transmembrane domain GPCRs. Serotonin$_{1A}$ receptors represent one of the largest, evolutionarily ancient, and highly conserved families of seven transmembrane GPCRs and is the most extensively studied of the serotonin receptors for a number of reasons [10]. Serotonin$_{1A}$

Abbreviations: 5-HT, 5-hydroxytryptamine (serotonin); AC, adenylyl cyclase; cAMP, adenosine 3′,5′-cyclic monophosphate; CD, cytochalasin D; DMSO, dimethyl sulphoxide; ERM, ezrin/radixin/moesin; Fsk, forskolin; GPCR, G-protein coupled receptor; H-89, N-[2-(*p*-bromocinnamylamino)ethyl]-5-isoquinolinesulfonamide; IBMX, 3-isobutyl-1-methylxanthine; Jas, jasplakinolide; LatA, latrunculin A; PDZ, PSD95/DlgA/ZO-1; PKA, protein kinase A

* Corresponding author. Tel.: +91 40 2719 2578; fax: +91 40 2716 0311.
E-mail address: amit@ccmb.res.in (A. Chattopadhyay).

0005-2736/$ – see front matter © 2011 Elsevier B.V. All rights reserved.
doi:10.1016/j.bbamem.2011.04.001

receptors are known to play a key role in the generation and modulation of various cognitive, developmental and behavioral functions. Agonists and antagonists of the serotonin$_{1A}$ receptor have been shown to possess potential therapeutic effects in anxiety- or stress-related disorders. As a result, the serotonin$_{1A}$ receptor serves as an important target in the development of therapeutic agents for neuropsychiatric disorders such as anxiety and depression. In addition, serotonin$_{1A}$ receptor mediated signaling has been implicated in various neurodevelopmental processes such as neurite growth and neuronal survival [11].

Upon binding serotonin, the serotonin$_{1A}$ receptor signals *via* Gα_i-mediated inhibition of AC, leading to the lowering of cAMP level and consequent downstream signaling [12–14]. The role of serotonin$_{1A}$ receptor signaling in various cellular processes such as DNA synthesis and regulation of signaling cascades has been identified previously [12 and references therein]. The metabolism of cellular cAMP is primarily determined by activities of AC and family of phosphodiesterases. Interestingly, variation in amplitude, duration, and gradient of intracellular cAMP is generated in response to different ligands [15]. In the context of GPCR signaling, cAMP-dependent protein kinase A (PKA) represent one of the primary components *via* which cAMP signaling is relayed further downstream. PKA is one of the well characterized protein kinases in eukaryotic cells, and serves as a model for the structure and function of cAMP binding proteins [15,16]. The binding of cAMP to PKA leads to the dissociation of the holoenzyme releasing its active catalytic subunit. The active catalytic subunit generates further downstream signaling by phosphorylation of multiple target proteins on serine and threonine residues [16–21].

Actin is one of the most abundant cytosolic proteins in eukaryotic cells and exists in both monomeric (globular or G-actin) and polymeric (filamentous or F-actin) forms. The two ends of F-actin are characterized by distinct growth rates; polymerization is relatively slow at the minus or 'pointed' end and fast at the plus or 'barbed' end. F-actin is maintained in cells in dynamic equilibrium with soluble G-actin. The extent of actin polymerization and depolymerization is orchestrated by a number of actin binding proteins (ABPs) in response to a variety of stimulus [22]. This provides a mechanism such that dynamic changes in the actin cytoskeleton, apart from providing structural stability to the cell, also act as a transducer in communicating signaling transients. While evidence of direct interaction of GPCRs with the actin cytoskeleton is lacking, several cytoskeleton-associated proteins have been reported to act as bridges by simultaneously interacting with GPCRs and the cytoskeleton. For example, calmodulin and other multi-motif proteins, such as those belonging to the ERM (ezrin/radixin/moesin) and PDZ (PSD95/DlgA/ZO-1) domain proteins, have been shown to interact with GPCRs [23–25]. This class of molecules, collectively termed as GPCR-interacting proteins (GIPs) are reported to be involved in trafficking and scaffolding of GPCRs on the plasma membrane, thereby regulating receptor signaling [26,27]. It has been previously reported for the serotonin$_{1A}$ receptor that the calcium binding protein calmodulin, which interacts with PDZ proteins, can bind to the third intracellular loop of the receptor [28].

In addition, cAMP/PKA signaling is known to induce significant changes in cellular architecture, such as dissolution of stress fibers and induction of stellate morphology in neurons and other cells. For example, increase in the intracellular cAMP level has been reported to cause significant changes in the cellular architecture of fibroblasts and neuronal cells [29–32]. Elevation of cAMP level has been suggested to activate PKA that results in inhibition of RhoA, a GTPase actively involved in actin filament dynamics and myosin phosphorylation [31]. Nonetheless, the role of cAMP/PKA mediated reorganization on the actin cytoskeleton has not been explored in terms of GPCR signaling.

In this context, we have previously reported that the signaling efficiency of the serotonin$_{1A}$ receptor, as monitored by its ability to reduce cellular cAMP level, is enhanced upon actin cytoskeleton destabilization [33]. Importantly, our results show that the lateral mobility (*i.e.*, mobile fraction) of serotonin$_{1A}$ receptors in the plasma membrane exhibits a *correlated* increase with receptor signaling upon actin cytoskeleton destabilization. Interestingly, we also observed an increase in receptor mobility when the cAMP level was increased independently by directly activating AC, implying a possible reorganization of the actin cytoskeleton with changes in cAMP level [33]. In this work, we have explored the effect of serotonin$_{1A}$ receptor signaling on the actin cytoskeleton organization in order to address the possibility of cytoskeletal reorganization upon GPCR signaling. To quantitatively monitor changes in the actin cytoskeletal network, we have employed advanced microscopy-based image reconstruction techniques. Our results suggest that the actin cytoskeleton is reorganized in response to serotonin$_{1A}$ receptor signaling. In addition, we show that reorganization of the actin cytoskeleton is strongly dependent on cAMP level, and is mediated by activation of PKA.

2. Materials and methods

2.1. Materials

$MgCl_2$, $CaCl_2$, cytochalasin D (CD), latrunculin A (LatA), serotonin (5-HT), penicillin, streptomycin and gentamicin sulfate were obtained from Sigma (St. Louis, MO). D-MEM/F-12 [Dulbecco's modified Eagle medium: nutrient mixture F-12 (Ham) (1:1)], fetal calf serum, and geneticin (G 418) were from Invitrogen Life Technologies (Carlsbad, CA). Alexa Fluor 546 conjugated phalloidin, Alexa Fluor 488 conjugated Dnase1 and jasplakinolide (Jas) were obtained from Molecular Probes (Eugene, OR). Forskolin, IBMX and H-89 were obtained from Calbiochem (San Diego, CA). Cyclic [^{3}H]AMP assay kit was purchased from Amersham Biosciences (Buckinghamshire, U.K.). All other chemicals used were of the highest available purity. Water was purified through a Millipore (Bedford, MA) Milli-Q system and used throughout.

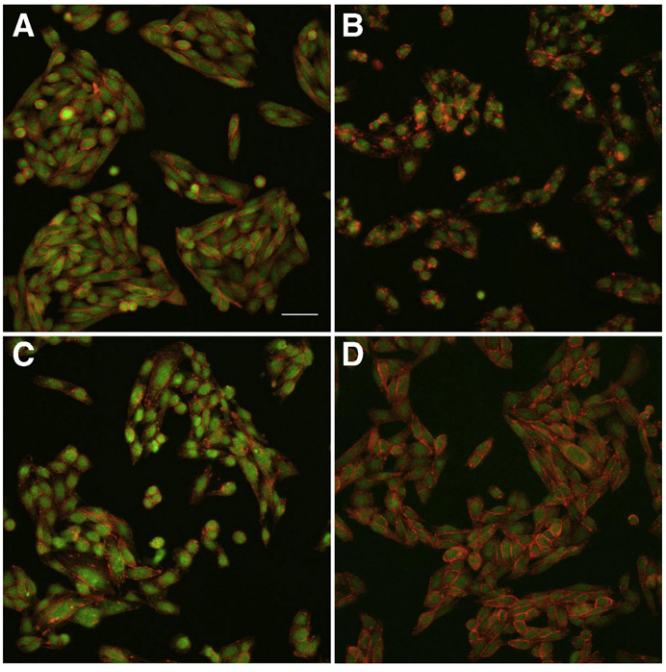

Fig. 1. Overall actin organization in CHO-5-HT$_{1A}$R cells treated with actin reorganizing agents. Cells cultured in monolayers on coverslips were fixed and F- and G-actin were stained with Alexa Fluor 546-phalloidin (red) and Alexa Fluor 488-Dnase1 (green), respectively. Imaging was performed with a 20×/0.75 NA objective. Panel A shows representative image of control (untreated) cells, while panels B–D correspond to cells treated with CD, LatA and Jas, respectively. The scale bar represents 50 μm. See Materials and methods for other details.

2.2. Methods

2.2.1. Cells, cell culture and treatments

CHO-K1 cells stably expressing the serotonin$_{1A}$ receptor (~10^5 receptors/cell) (referred to as CHO-5-HT$_{1A}$R) were used. Cells were grown in D-MEM/F-12 (1:1) supplemented with 2.4 g/l of sodium bicarbonate, 10% fetal calf serum, 60 μg/ml penicillin, 50 μg/ml streptomycin, and 50 μg/ml gentamicin sulfate in a humidified atmosphere with 5% CO_2 at 37 °C. CHO-5-HT$_{1A}$R cells were maintained in the above mentioned conditions with 200 μg/ml geneticin. Stock solutions of CD, LatA, Jas, Fsk and H-89 were made in DMSO. Further concentrations for treatments were prepared upon dilution of the stock in buffer A (phosphate buffered saline containing 1 mM $CaCl_2$ and 0.5 mM $MgCl_2$). The final concentration of DMSO was 0.5% (v/v) in all cases except when serotonin was used. Serotonin was directly dissolved in buffer A to make the desired concentrations. The concentrations used were: CD (10 μM), LatA (0.2 μM), Jas (0.2 μM), Fsk (10 μM), H-89 (3 μM) and 5-HT (10 μM). Treatments were carried out for 30 min at room temperature (~23 °C) in all cases.

2.2.2. F- and G-actin labeling of cells

CHO-5-HT$_{1A}$R cells were plated at a density of 10^4 cells on glass coverslips and were grown in D-MEM/F-12 medium for 24 h. The coverslips were washed with buffer A, and cells were treated as specified for 30 min at room temperature (~23 °C). Following treatment, cells were washed with buffer A and fixed with 3.5% (v/v) formaldehyde for 10 min. Subsequent permeabilization of cells was carried out in presence of 0.5% (v/v) Triton X-100 and 0.05% (v/v) Tween-20 for 6 min. Cells were washed and stained with Alexa Fluor 546 conjugated phalloidin (for F-actin) and Alexa Fluor 488 conjugated Dnase1 (for G-actin) for 1 h prior to mounting. Since Jas is known to competitively inhibit phalloidin binding to F-actin [34], permeabilized cells were washed multiple times with buffer A upon Jas treatment, prior to labeling with Alexa Fluor 546 conjugated phalloidin.

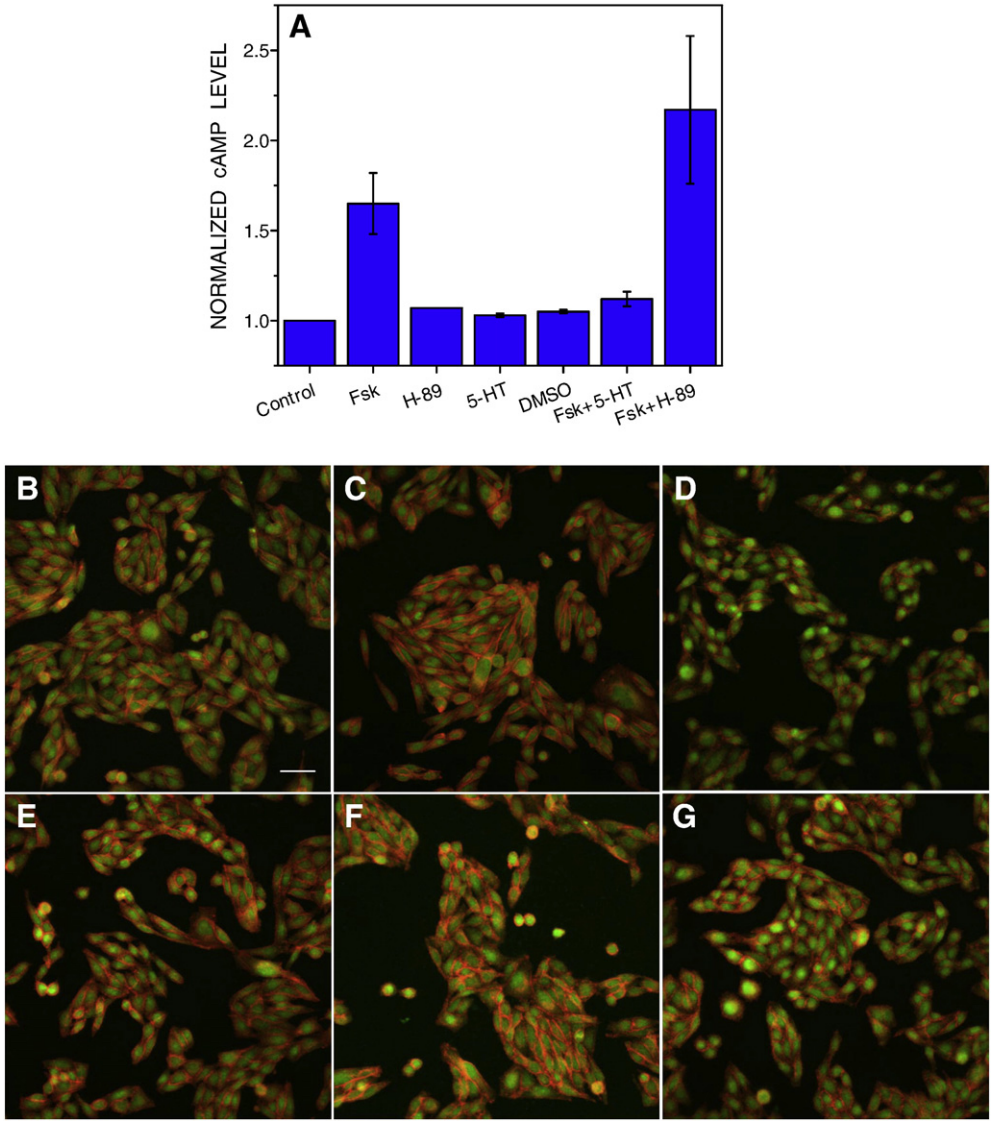

Fig. 2. Normalized cAMP level in CHO-5-HT$_{1A}$R cells upon treatment with agents involved in serotonin$_{1A}$ receptor signaling are shown in panel A. Data were normalized with respect to cAMP level estimated in control cells and represent normalized means ± SE of at least three independent measurements. Panels B–G show actin organization in CHO-5-HT$_{1A}$R cells treated with agents involved in serotonin$_{1A}$ receptor signaling. F- and G-actin were stained with Alexa Fluor 546-phalloidin (red) and Alexa Fluor 488-Dnase1 (green), respectively. Imaging was performed with a 20×/0.75 NA objective. Panel B shows representative image of cells treated with DMSO, while panels C–G correspond to cells treated with 5-HT, Fsk, Fsk + 5-HT, H-89 and Fsk + H-89, respectively. The scale bar represents 50 μm. See Materials and methods for other details.

2.2.3. Fluorescence microscopy

All images were acquired on an inverted Zeiss LSM 510 Meta confocal microscope (Jena, Germany). Alexa Fluor 546 conjugated phalloidin imaging was performed upon excitation at 543 nm and emission was collected from 565 to 615 nm. Alexa Fluor 488 conjugated Dnase1 was excited at 488 nm and emission was collected from 500 to 530 nm. Low magnification images were acquired with a 20×/0.75 NA objective with an open pinhole. High magnification images were acquired with a 63×/1.4 NA oil immersion objective under 1 airy condition for Alexa Fluor 546 conjugated phalloidin (93 μm, giving a fixed z-slice of 0.32 μm). The images shown in Figs. 3, 5 and 7 represent the projected sections from the base (attached to the cover slip) to ~3 μm (10–12 sections) into the cell.

2.2.4. Estimation of cAMP level in cells

The ability of the agonist to downregulate the forskolin-stimulated increase in cAMP level in cells was assessed as described previously [33]. Briefly, CHO-5-HT_{1A}R cells were plated at a density of 10^4 cells per well in 24-well plates and grown in D-MEM/F-12 medium for 24 h. All treatments were performed for 30 min in buffer A. Cells were rinsed with PBS and incubated with 10 μM Fsk at 23 °C for 30 min in serum-free medium. The phosphodiesterase inhibitor IBMX (50 μM) was present during this treatment. After incubation, cells were lysed in 10 mM Tris and 5 mM EDTA, pH 7.4 buffer. Cell lysates were boiled for 15–20 min and spun for 15 min in a refrigerated Eppendorf 5417R centrifuge at ~25,000 *g* to remove precipitated proteins. The amount of cAMP in an aliquot of the supernatant was estimated using the [^{3}H] cAMP assay, based on the protein binding method described previously [35]. Relative cAMP level was calculated upon normalization of the data to the cAMP content in control cells.

2.2.5. Image and data analysis

Iso-surface (*i.e.*, a contour made upon joining voxels of equal fluorescence intensity) generation of selected sections was performed using Bitplane software (Bitplane AG, Zurich, Switzerland; see http://www.bitplane.com/go/products/imaris for details). Iso-surfaces were generated upon thresholding of images followed by applying a Gaussian filter. The estimated volumes enclosed by iso-surfaces were normalized to the projected area of the cells for the given field. The projected area was determined manually by utilizing the software provided with LSM 510 Meta Confocal microscope (Zeiss, Jena, Germany). Further plotting and analysis of the estimated parameters were carried out using Origin software version 7.0 (OriginLab Corp., Northampton, MA) and Microsoft Excel 2007 (Redmond, WA). Significance levels were estimated by Student's two-tailed unpaired *t*-test using Graphpad Prism software version 4.0 (San Diego, CA).

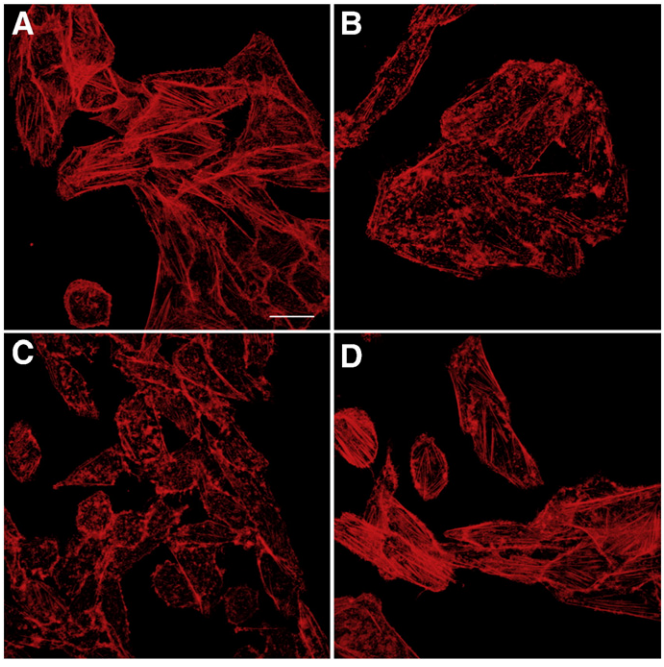

Fig. 3. Organization of the actin cytoskeleton in CHO-5-HT_{1A}R cells treated with actin reorganizing agents. The actin cytoskeleton was stained with Alexa Fluor 546-phalloidin and a projection of 10–12 sections from the base (~3 μm from the coverslip into the cell) is shown. Panel A shows a projected image for cells treated with DMSO, while panels B–D correspond to cells treated with CD, LatA and Jas, respectively. All treatments were carried out in buffer A for 30 min. The scale bar represents 20 μm. See Materials and methods for other details.

3. Results

3.1. Quantitative estimate of F-actin organization

In order to quantitatively estimate the extent of actin reorganization, CHO-5-HT_{1A}R cells were treated with actin-reorganizing agents

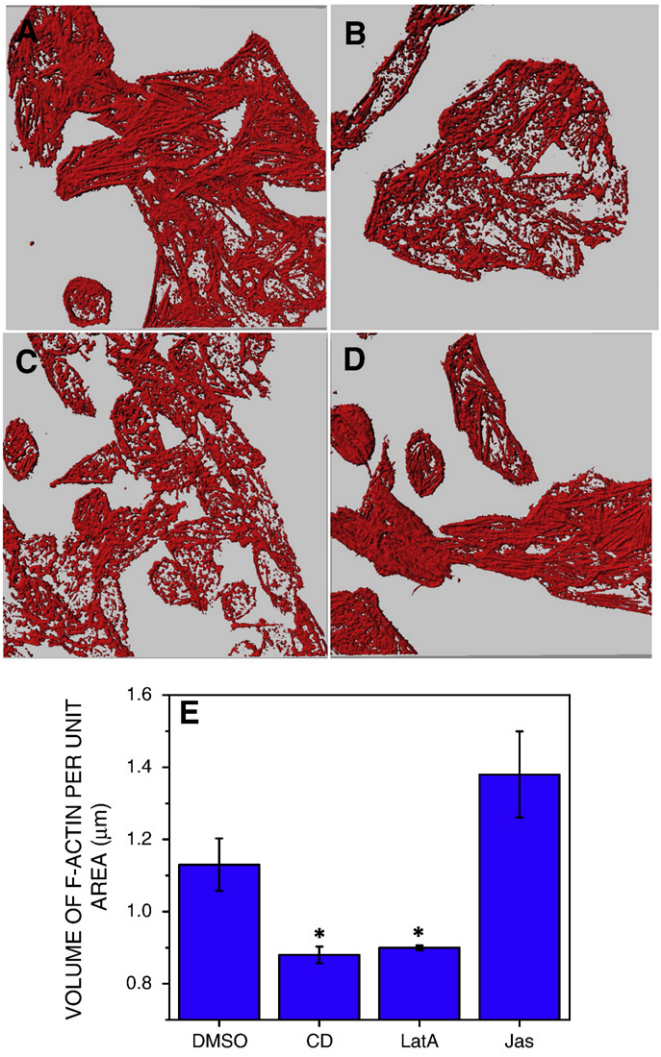

Fig. 4. Iso-surface generation and quantitation of F-actin. Iso-surfaces of the same selection of sections as shown in Fig. 3 were generated using the Iso-surface tool in Imaris. The volume formed by the generated iso-surface was normalized to the projected area of cells in the field using the software provided with LSM 510 Meta confocal microscope. Panel A shows the iso-surface image of cells treated with DMSO, while panels B–D correspond to cells treated with CD, LatA and Jas, respectively. Panel E shows the quantitative measure of F-actin. Data represent means ± S.E. of at least three independent and matched measurements performed on different days with >8 cells in the field (* corresponds to a p-value<0.05, compared to DMSO treated cells). See Materials and methods for other details.

and labeled with Alexa Fluor 546-phalloidin and Alexa Fluor 488-Dnase1. Phalloidin and Dnase1 were utilized to simultaneously label F- and G-actin [36,37]. We employed actin-reorganizing agents, namely, LatA, CD and Jas, to induce reorganization of the cellular actin cytoskeleton. While LatA and CD are known to induce F-actin depolymerization, Jas is known to induce F-actin formation [34,38,39]. As shown in Fig. 1, treatment of cells with LatA and CD resulted in fragmentation of filamentous actin (Fig. 1B and C). Treatment with Jas, on the other hand, led to an increase in the F-actin content (Fig. 1D). To explore possible reorganization of the actin cytoskeleton in response to serotonin$_{1A}$ receptor signaling, we monitored actin reorganization induced by agents involved in such signaling. As mentioned above, ligand-mediated activation of the serotonin$_{1A}$ receptor leads to a reduction of cellular cAMP level [12]. Since the basal level of cAMP are often low to monitor further reduction, Fsk (a direct activator of AC) is commonly employed to increase cAMP level prior to ligand stimulation. We used H-89 to monitor the effect of blocking downstream signaling mediated *via* the cAMP/PKA pathway on the actin cytoskeleton. H-89 is known to bind to the catalytic subunit of PKA in a competitive fashion against ATP and inhibits kinase activity [40]. The estimated cAMP levels in cells treated with agents involved in serotonin$_{1A}$ receptor signaling are shown in Fig. 2A, and the corresponding actin organization is shown in Fig. 2B–G. While no discernable change was observed in the case of cells treated with DMSO, serotonin or H-89 (Fig. 2B, C and F respectively), we observed a reduction of F-actin content in cells treated with Fsk (Fig. 2D) in agreement with depolymerization of F-actin in the presence of high cAMP level (shown in Fig. 2A). The depolymerization of F-actin was reversed either in cells treated with serotonin and Fsk, or in cells treated with Fsk and H-89 (Fig. 2E and G). These observations indicate that while serotonin$_{1A}$ receptor signaling reduces cAMP level (Fig. 2A), the destabilization of F-actin at high cAMP level is brought about by an activated PKA dependent pathway (see later text). Interestingly, the cAMP level was found to be higher in the case of cells treated with Fsk and H-89, compared to cells treated with Fsk alone (Fig. 2A). This could possibly be due to the competitive nature of H-89 binding to PKA, resulting in an increase in the content of free cAMP available in cells.

In order to monitor these changes in the actin cytoskeleton in a quantitative fashion, we estimated the ratio of F-actin to the content of G-actin (F/G ratio). The integrated fluorescence intensities originating from a group of cells in the two emission channels of the microscope (the red and green channels, corresponding to F- and G-actin) were utilized to determine the F/G ratio. Unfortunately, while these measurements were statistically robust due to the collection from a large number of cells in the field, the F/G ratio exhibited low dynamic range and high variance (percent deviation ~50; data not shown), possibly due to intrinsic variation in the cellular population. To circumvent the above problems, we performed high magnification imaging of F-actin followed by image reconstruction. Images were acquired at 63× magnification and 10–12 sections (z-slice of 0.32 μm) were selected from the base (~3 μm from the surface of the cell attached to the coverslip) and an iso-surface of F-actin (primarily representing the ventral stress fibers [41]) was generated. The projected images of cells treated with actin reorganizing agents are shown in Fig. 3, and the

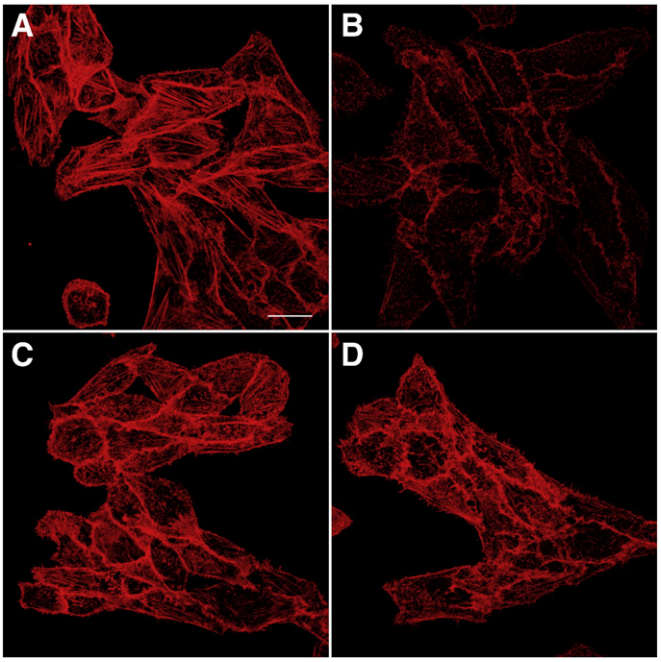

Fig. 5. Projected images of cellular F-actin upon increase in cellular cAMP. The actin cytoskeleton was stained with Alexa Fluor 546-phalloidin and a projection of 10–12 sections from the base (~3 μm from the coverslip into the cell) is shown. Panel A shows a projected image for cells treated with DMSO, while panels B–D correspond to cells treated with Fsk, H-89 and Fsk + H-89, respectively. All treatments were carried out in buffer A for 30 min. The scale bar represents 20 μm. See Materials and methods for other details.

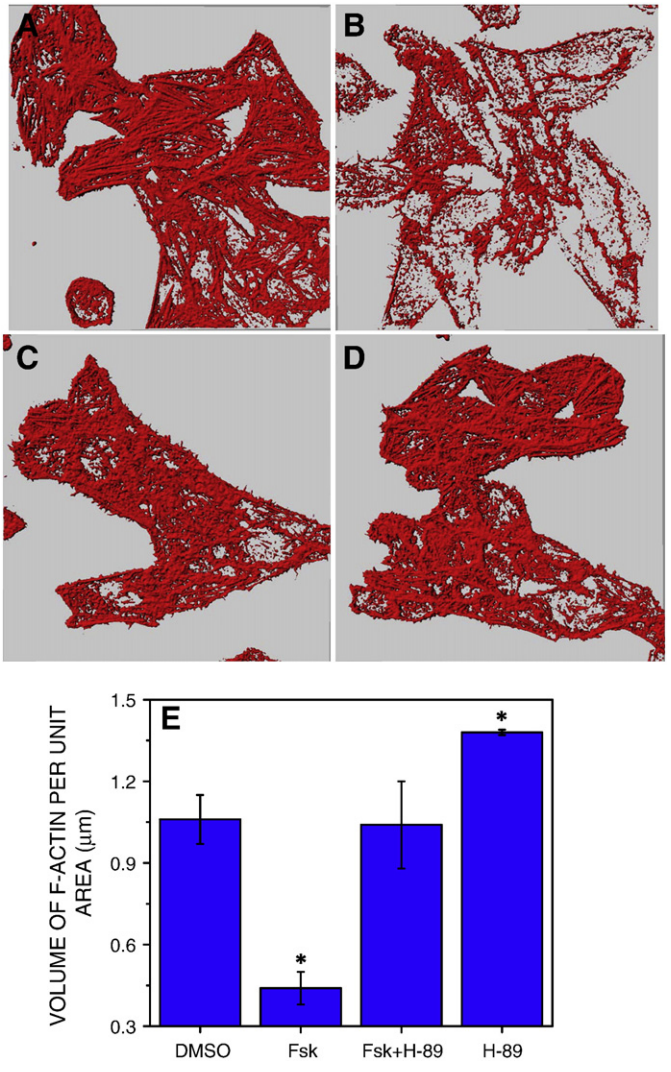

Fig. 6. Loss of F-actin upon increase of cellular cAMP. Iso-surfaces of the same selection of sections as shown in Fig. 5 were generated using the Iso-surface tool in Imaris (as described in Fig. 4). Panel A shows the iso-surface image of cells treated with DMSO, while panels B–D correspond to cells treated with Fsk, H-89 and Fsk + H-89, respectively. The quantitative measure of F-actin is shown in panel E. Data represent means ± S.E. of at least three independent and matched measurements performed on different days with >8 cells in the field (* corresponds to a p-value<0.05, compared to DMSO treated cells). See Materials and methods for other details.

corresponding iso-surface images are shown in Fig. 4A–D. We observed that the total volume enclosed by the iso-surface, normalized to the projected area of the cells, provides best estimate of changes in F-actin content. The estimate of F-actin derived this way (averaged over ~25 cells) is shown in Fig. 4E. As can be seen in Fig. 4E, treatments leading to a loss of F-actin (CD and LatA) displayed a significant reduction in the estimated parameter, whereas treatment with Jas exhibited an increase. In contrast to estimates of actin reorganization using low magnification imaging, estimation of F-actin using high magnification imaging by this approach improved the dynamic range and overall reproducibility.

3.2. Increase in cAMP level leads to a reduction of F-actin

To monitor changes in F-actin when cAMP level is elevated, we quantitated F-actin in cells treated with Fsk. As mentioned earlier, Fsk is a direct activator of AC and leads to an increase in cellular cAMP level. Figs. 5 and 6 show that elevation of cAMP level by Fsk leads to a reduction of F-actin. To further probe the mechanism of actin depolymerization mediated by increased level of cAMP (induced by Fsk), we used H-89, an inhibitor of PKA. Interestingly, inhibiting PKA by H-89 rescues F-actin depolymerization to a large extent. These observations imply that elevated cAMP level results in actin depolymerization, mediated by activation of PKA. Importantly, H-89 treatment alone led to an increase in F-actin content, probably by inhibiting basal PKA mediated signaling in these cells. Interestingly, the reduction in F-actin brought about by elevated cAMP level appears to reorganize the cytoskeleton differently than observed for actin depolymerizing agents like CD and LatA. While CD and LatA tend to fragment F-actin into foci, high level of cAMP results in an overall reduction in F-actin without the generation of foci (see Figs. 3B, C and 5B, and Figs. 4B, C and 6B).

3.3. Reorganization of the actin cytoskeleton upon serotonin$_{1A}$ receptor activation

To monitor whether activation of the serotonin$_{1A}$ receptor and subsequent signaling bring about changes in the actin cytoskeleton, we estimated F-actin upon treatment of cells with serotonin (Figs. 7 and 8). Stimulation of cells with serotonin led to an increase in F-actin compared to control (untreated) cells (Fig. 8F). Interestingly, we observed that treatment of cells with DMSO led to an increase in F-actin. Importantly, the reduction of F-actin brought about by stimulation of cells with Fsk (Fig. 7D) was recovered when cells were treated with Fsk in the presence of serotonin (Fig. 7E). The increase in F-actin content upon serotonin treatment suggests that serotonin$_{1A}$ receptor signaling is involved in reduction of basal cAMP level, driving cellular actin polymerization. However, the assay utilized by us to estimate cAMP level was unable to differentiate any change in cAMP level between control and serotonin treated cells (Fig. 2A). This could possibly be due to the inherent insensitivity of the assay at low cAMP concentrations. Taken together, our results imply that signaling by the serotonin$_{1A}$ receptor mediated through cAMP/PKA could dynamically modulate the actin cytoskeleton by lowering cAMP level.

4. Discussion

The actin cytoskeleton is involved in a multitude of cellular responses in addition to providing structural support. While the role of the actin cytoskeleton in cellular processes such as trafficking and motility has been intensely studied [42], the reorganization of the actin cytoskeleton upon GPCR signaling has been rarely addressed. In this work, we present a quantitative estimate of actin reorganization upon activation of the serotonin$_{1A}$ receptor. Our results suggest that elevated cAMP level leads to a reduction in F-actin content through activation of PKA. In addition, we report that serotonin$_{1A}$ receptor signaling results in an increase in F-actin content in cells, possibly due to the reduction of basal cAMP level (Fig. 8). To monitor the changes in the actin cytoskeleton in a quantitative fashion, we have developed an approach based on high magnification imaging of F-actin in cells, followed by image reconstruction. With the benefit of an improved dynamic range and low variance of the acquired data, we were able to ascribe reorganization of the actin cytoskeleton upon alteration of cAMP level (which is mediated by serotonin$_{1A}$ receptor signaling).

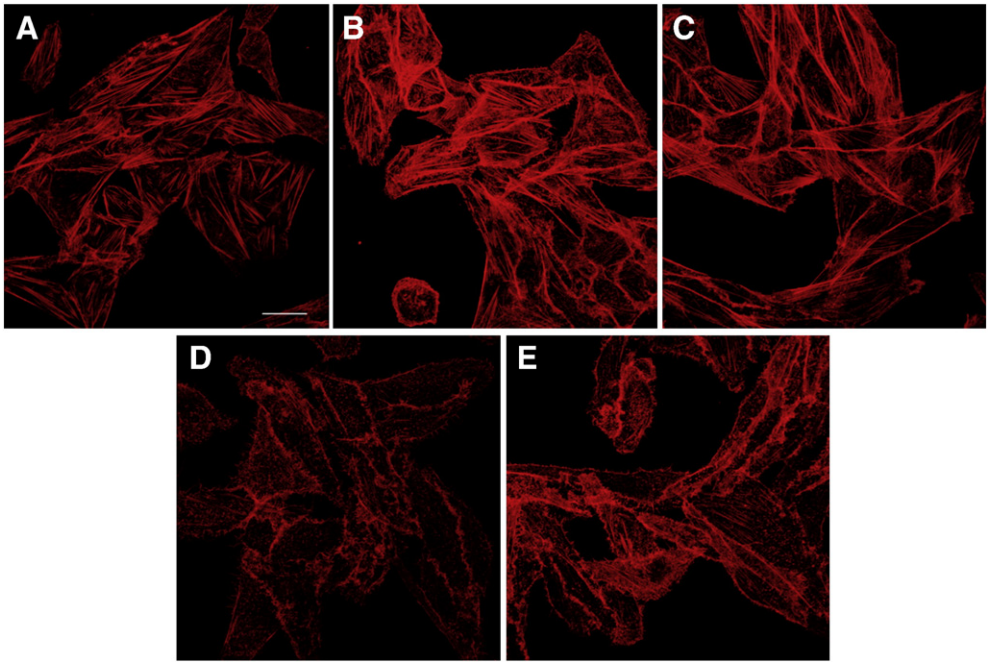

Fig. 7. Projected images of cellular F-actin in CHO-5-HT$_{1A}$R cells treated with agents involved in serotonin$_{1A}$ receptor signaling. The actin cytoskeleton was stained with Alexa Fluor 546-phalloidin and a projection of 10–12 sections from the base (~3 μm from the coverslip into the cell) is shown. Panel A shows a projected image for control (untreated) cells, while panels B–E correspond to cells treated with DMSO, 5-HT, Fsk, and Fsk + 5-HT, respectively. All treatments were carried out in buffer A for 30 min. The scale bar represents 20 μm. See Materials and methods for other details.

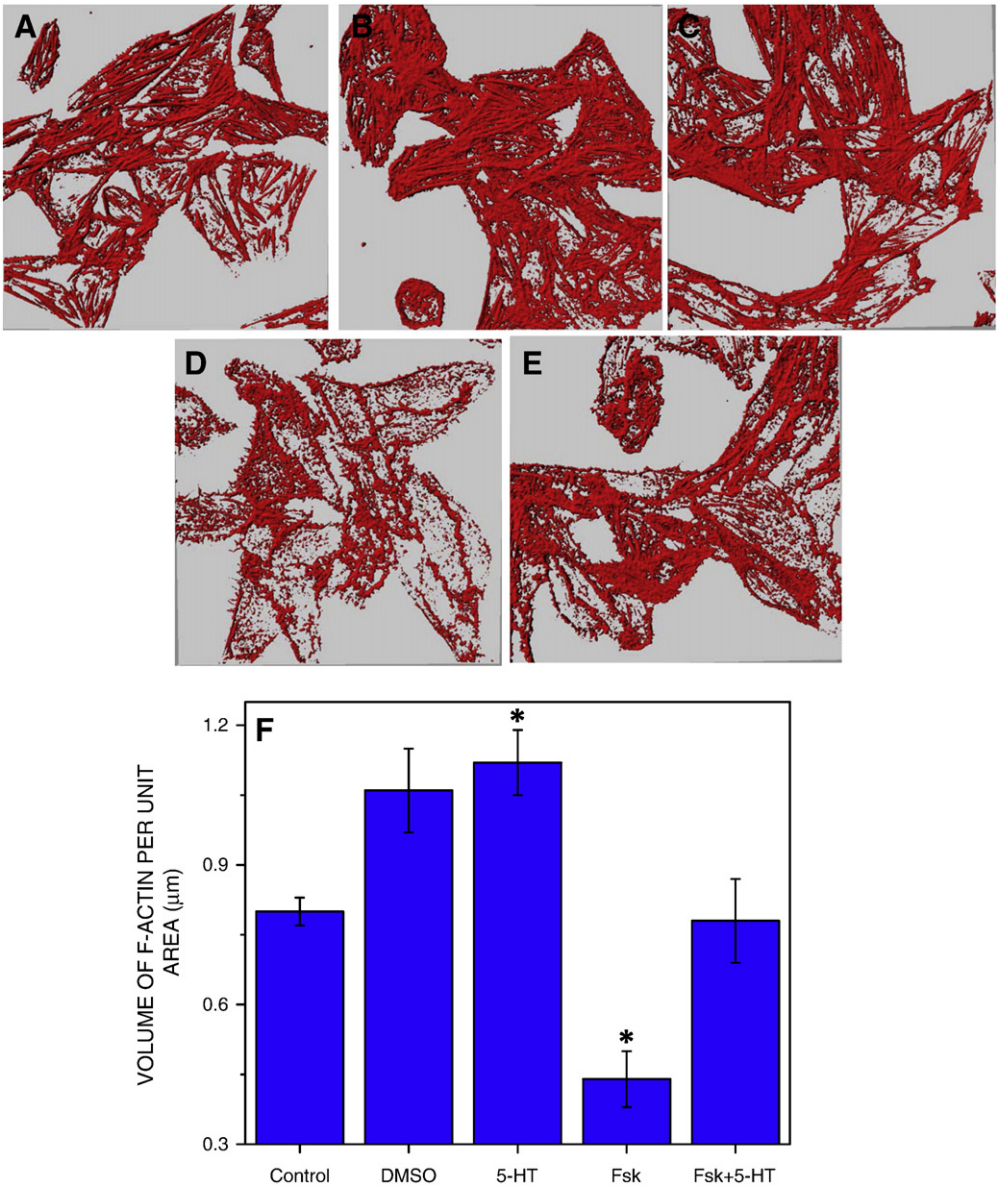

Fig. 8. F-actin destabilization is inhibited in the presence of serotonin. Iso-surfaces of the same selection of sections as shown in Fig. 7 were generated using the Iso-surface tool in Imaris (as described in Fig. 4). Panel A shows a projected image for control (untreated) cells, while panels B–E correspond to cells treated with DMSO, 5-HT, Fsk, and Fsk + 5-HT, respectively. The quantitative measure of F-actin is shown in panel F. Data represent means ± S.E. of at least three independent and matched measurements performed on different days with >8 cells in the field (* corresponds to a p-value<0.05, compared to control cells). See Materials and methods for other details.

Interestingly, we have earlier reported that the mobility and oligomerization of serotonin$_{1A}$ receptors in the plasma membrane is regulated by the integrity of the underlying actin cytoskeleton [33,43–45]. We previously observed a progressive increase in the fraction of mobile receptors, estimated from FRAP measurements with increasing actin depolymerization [33]. Significantly, the signaling efficiency of the receptor (defined as the extent of reduction of cAMP in Fsk stimulated cells for a given ligand concentration) exhibited a remarkable correlation to the increase in mobile fraction under these conditions [33]. These results, in combination with our present data, generate the following interesting aspects of serotonin$_{1A}$ receptor signaling: (i) serotonin$_{1A}$ receptor signaling leads to an increase in F-actin content by reducing cAMP level; (ii) increase in cAMP level leads to F-actin destabilization; and (iii) destabilization of F-actin results in an increase in receptor mobility (mobile fraction of receptors) with a correlated increase in receptor signaling. In the continuous presence of extracellular ligand, the serotonin$_{1A}$ receptor, cAMP level and the actin cytoskeleton network could be involved in a negative feedback cycle capable of generating oscillatory response [46]. These responses could be further modulated *in vivo*, depending upon the presence of extracellular ligand gradients, as well as differential structural organization of the underlying cytoskeleton in specialized cells such as neurons. Interestingly, differential mobility of proteins between navigating and non-navigating growth cones in neurons, possibly due to the differences in the sub-membraneous actin cytoskeleton, has been previously observed [47]. In addition, with growing evidence in favor of localized signaling by cAMP [48], our results raise an interesting possibility of a dynamic system involving the actin cytoskeleton, cAMP level and the serotonin$_{1A}$ receptor. We note that the above system, in the presence of extracellular serotonin, could be driven by a local negative feedback loop. According to this model, a localized increase in cAMP level can reorganize the actin cytoskeleton, leading to increased receptor mobility and therefore signaling by the serotonin$_{1A}$ receptor, which in effect would reduce cAMP level (see Fig. 9). Interestingly, ligand gradient or cAMP dependent growth of neurons have been reported earlier [49,50].

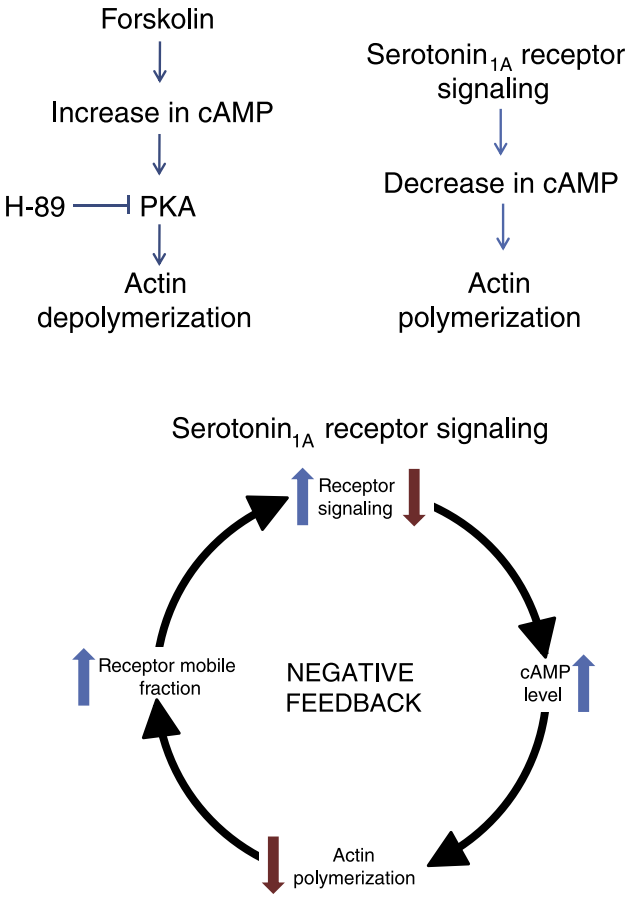

Fig. 9. A schematic representation depicting the changes brought about in the actin cytoskeleton by cellular cAMP level. Dynamics of the actin cytoskeleton (F-actin) is not only sensitive to cAMP level, but also requires active PKA. In this context, if the modulation in receptor mobility and signaling upon cytoskeletal destabilization [33] are taken into account, the receptor, cellular cAMP and the actin cytoskeleton appear to form a negative feedback loop. Such a feedback loop would, in principle, be capable of generating local oscillatory response. See text for further discussion.

In summary, we report here quantitative measurements on the changes in F-actin upon signaling by the serotonin$_{1A}$ receptor. We observe that alterations in cAMP level regulate the organization of F-actin. It has been recently reported that activation of the luteinizing hormone receptor leads to a transient depolymerization of actin [51]. Interestingly, the luteinizing hormone receptor is coupled to Gα_s and leads to an increase in cAMP level. These results suggest that cellular level of cAMP significantly influences the balance between polymerized and monomeric forms of actin. The dynamic reorganization of the actin cytoskeleton may represent an important determinant in GPCR signaling.

Acknowledgements

This work was supported by the Council of Scientific and Industrial Research, Government of India. S.G. and R.S. thank Council of Scientific and Industrial Research for the award of Senior Research Fellowships. A.C. is an Adjunct Professor at the Special Centre for Molecular Medicine of Jawaharlal Nehru University (New Delhi, India) and Indian Institute of Science Education and Research (Mohali, India), and Honorary Professor at the Jawaharlal Nehru Centre for Advanced Scientific Research (Bangalore, India). A.C. gratefully acknowledges J.C. Bose Fellowship (Dept. of Science and Technology, Govt. of India). We thank Nandini Rangaraj for useful discussions, and members of our laboratory for critically reading the manuscript.

References

[1] K.L. Pierce, R.T. Premont, R.J. Lefkowitz, Seven-transmembrane receptors, Nat. Rev. Mol. Cell Biol. 3 (2002) 639–650.
[2] D.M. Rosenbaum, S.G.F. Rasmussen, B.K. Kobilka, The structure and function of G-protein-coupled receptors, Nature 459 (2009) 356–363.
[3] M.J. Marinissen, J.S. Gutkind, G-protein-coupled receptors and signaling networks: emerging paradigms, Trends Pharmacol. Sci. 22 (2001) 368–376.
[4] Y. Zhang, M.E. DeVries, J. Skolnick, Structure modeling of all identified G protein-coupled receptors in the human genome, PLoS Comput. Biol. 2 (2006) e13.
[5] M.C. Lagerström, H.B. Schiöth, Structural diversity of G protein-coupled receptors and significance for drug discovery, Nat. Rev. Drug Discov. 7 (2008) 339–357.
[6] R. Heilker, M. Wolff, C.S. Tautermann, M. Bieler, G-protein-coupled receptor-focused drug discovery using a target class platform approach, Drug Discov. Today 14 (2009) 231–240.
[7] S.H. Lin, O. Civelli, Orphan G protein-coupled receptors: targets for new therapeutic interventions, Ann. Med. 36 (2004) 204–214.
[8] U. Gether, Uncovering molecular mechanisms involved in activation of G protein-coupled receptors, Endocr. Rev. 21 (2000) 90–113.
[9] W.M. Oldham, H.E. Hamm, Structural basis of function in heterotrimeric G proteins, Q. Rev. Biophys. 39 (2006) 117–166.
[10] T.J. Pucadyil, S. Kalipatnapu, A. Chattopadhyay, The serotonin$_{1A}$ receptor: a representative member of the serotonin receptor family, Cell. Mol. Neurobiol. 25 (2005) 553–580.
[11] A.D. Fricker, C. Rios, L.A. Devi, I. Gomes, Serotonin receptor activation leads to neurite outgrowth and neuronal survival, Brain Res. Mol. Brain Res. 138 (2005) 228–235.
[12] J.R. Raymond, Y.V. Mukhin, T.W. Gettys, M.N. Garnovskaya, The recombinant 5-HT$_{1A}$ receptor: G protein coupling and signalling pathways, Br. J. Pharmacol. 127 (1999) 1751–1764.
[13] G.J. Della Rocca, Y.V. Mukhin, M.N. Garnovskaya, Y. Daaka, G.J. Clark, L.M. Luttrell, R.J. Lefkowitz, J.R. Raymond, Serotonin 5-HT$_{1A}$ receptor-mediated Erk activation requires calcium/calmodulin-dependent receptor endocytosis, J. Biol. Chem. 274 (1999) 4749–4753.
[14] S.-C. Hsiung, A. Tin, H. Tamir, T.F. Franke, K.-P. Liu, Inhibition of 5-HT$_{1A}$ receptor-dependent cell survival by cAMP/protein kinase A: role of protein phosphatase 2A and Bax, J. Neurosci. Res. 86 (2008) 2326–2338.
[15] S. Seino, T. Shibasaki, PKA-dependent and PKA-independent pathways for cAMP-regulated exocytosis, Physiol. Rev. 85 (2005) 1303–1342.
[16] S.S. Taylor, C. Kim, D. Vigil, N.M. Haste, J. Yang, J. Wu, G.S. Anand, Dynamics of signaling by PKA, Biochim. Biophys. Acta 1754 (2005) 25–37.
[17] M.C. Martin, L.A. Allan, M. Lickrish, C. Sampson, N. Morrice, P.R. Clarke, Protein kinase A regulates caspase-9 activation by Apaf-1 downstream of cytochrome *c*, J. Biol. Chem. 280 (2005) 15449–15455.
[18] A.J. Shaywitz, M.E. Greenberg, CREB: a stimulus-induced transcription factor activated by a diverse array of extracellular signals, Annu. Rev. Biochem. 68 (1999) 821–861.
[19] P.J. Stork, J.M. Schmitt, Crosstalk between cAMP and MAP kinase signaling in the regulation of cell proliferation, Trends Cell Biol. 12 (2002) 258–266.
[20] N. Takahashi, T. Tetsuka, H. Uranishi, T. Okamoto, Inhibition of the NF-κB transcriptional activity by protein kinase A, Eur. J. Biochem. 269 (2002) 4559–4565.
[21] H. Usui, R. Inoue, O. Tanabe, Y. Nishito, M. Shimizu, H. Hayashi, H. Kagamiyama, M. Takeda, Activation of protein phosphatase 2A by cAMP-dependent protein kinase-catalyzed phosphorylation of the 74-kDa B" (δ) regulatory subunit in vitro and identification of the phosphorylation sites, FEBS Lett. 430 (1998) 312–316.
[22] C.G. dos Remedios, D. Chhabra, M. Kekic, I.V. Dedova, M. Tsubakihara, D.A. Berry, N.J. Nosworthy, Actin binding proteins: regulation of cytoskeletal microfilaments, Physiol. Rev. 83 (2003) 433–473.
[23] S.L. Ritter, R.A. Hall, Fine-tuning of GPCR activity by receptor-interacting proteins, Nat. Rev. Mol. Cell Biol. 10 (2009) 819–830.
[24] E. Jacoby, R. Bouhelal, M. Gerspacher, K. Seuwen, The 7 TM G-protein-coupled receptor target family, ChemMedChem 1 (2006) 760–782.
[25] J. Bockaert, P. Marin, A. Dumuis, L. Fagni, The 'magic tail' of G protein-coupled receptors: an anchorage for functional protein networks, FEBS Lett. 546 (2003) 65–72.
[26] N. Tilakaratne, P.M. Sexton, G-protein-coupled receptor-protein interactions: basis for new concepts on receptor structure and function, Clin. Exp. Pharmacol. Physiol. 32 (2005) 979–987.
[27] J. Bockaert, G. Roussignol, C. Bécamel, S. Gavarini, L. Joubert, A. Dumuis, L. Fagni, P. Marin, GPCR-interacting proteins (GIPs): nature and functions, Biochem. Soc. Trans. 32 (2004) 851–855.
[28] J.H. Turner, A.K. Gelasco, J.R. Raymond, Calmodulin interacts with the third intracellular loop of the serotonin 5-hydroxytryptamine$_{1A}$ receptor at two distinct sites: putative role in receptor phosphorylation by protein kinase C, J. Biol. Chem. 279 (2004) 17027–17037.
[29] N.J.C. Lamb, A. Fernandez, M.A. Conti, R. Adelstein, D.B. Glass, W.J. Welch, J.R. Feramisco, Regulation of actin microfilament integrity in living nonmuscle cells by the cAMP-dependent protein kinase and the myosin light chain kinase, J. Cell Biol. 106 (1988) 1955–1971.
[30] J.-M. Dong, T. Leung, E. Manser, L. Lim, cAMP-induced morphological changes are counteracted by the activated RhoA small GTPase and the Rho kinase ROKα, J. Biol. Chem. 273 (1998) 22554–22562.
[31] A.K. Howe, Regulation of actin-based cell migration by cAMP/PKA, Biochim. Biophys. Acta 1692 (2004) 159–174.
[32] K. Szászi, K. Kurashima, K. Kaibuchi, S. Grinstein, J. Orlowski, Role of the cytoskeleton in mediating cAMP-dependent protein kinase inhibition of the epithelial Na^+/H^+ exchanger NHE3, J. Biol. Chem. 276 (2001) 40761–40768.

[33] S. Ganguly, T.J. Pucadyil, A. Chattopadhyay, Actin cytoskeleton-dependent dynamics of the human serotonin$_{1A}$ receptor correlates with receptor signaling, Biophys. J. 95 (2008) 451–463.
[34] M.R. Bubb, A.M.J. Senderowicz, E.A. Sausville, K.L.K. Duncan, E.D. Korn, Jasplakinolide, a cytotoxic natural product, induces actin polymerization and competitively inhibits the binding of phalloidin to F-actin, J. Biol. Chem. 269 (1994) 14869–14871.
[35] C. Nordstedt, B.B. Fredholm, A modification of a protein-binding method for rapid quantification of cAMP in cell-culture supernatants and body fluid, Anal. Biochem. 189 (1990) 231–234.
[36] G.C. Knowles, C.A.G. McCulloch, Simultaneous localization and quantification of relative G and F actin content: optimization of fluorescence labeling methods, J. Histochem. Cytochem. 40 (1992) 1605–1612.
[37] R.P. Haugland, W. You, V.B. Paragas, K.S. Wells, D.A. DuBose, Simultaneous visualization of G- and F-actin in endothelial cells, J. Histochem. Cytochem. 42 (1994) 345–350.
[38] P. Sampath, T.D. Pollard, Effects of cytochalasin, phalloidin, and pH on the elongation of actin filaments, Biochemistry 30 (1991) 1973–1980.
[39] I. Spector, N.R. Shochet, Y. Kashman, A. Groweiss, Latrunculins: novel marine toxins that disrupt microfilament organization in cultured cells, Science 214 (1983) 493–495.
[40] T. Chijiwa, A. Mishima, M. Hagiwara, M. Sano, K. Hayashi, T. Inoue, K. Naito, T. Toshioka, H. Hidaka, Inhibition of forskolin-induced neurite outgrowth and protein phosphorylation by a newly synthesized selective inhibitor of cyclic AMP-dependent protein kinase, *N*-[2-(*p*-bromocinnamylamino)ethyl]-5-isoquinolinesulfonamide (H-89), of PC12D pheochromocytoma cells, J. Biol. Chem. 265 (1990) 5267–5272.
[41] S. Pellegrin, H. Mellor, Actin stress fibres, J. Cell Sci. 120 (2007) 3491–3499.
[42] P.A. Janmey, The cytoskeleton and cell signaling: component localization and mechanical coupling, Physiol. Rev. 78 (1998) 763–781.
[43] S. Ganguly, P. Singh, R. Manoharlal, R. Prasad, A. Chattopadhyay, Differential dynamics of membrane proteins in yeast, Biochem. Biophys. Res. Commun. 387 (2009) 661–665.
[44] S. Ganguly, A. Chattopadhyay, Cholesterol depletion mimics the effect of cytoskeletal destabilization on membrane dynamics of the serotonin$_{1A}$ receptor: a zFCS study, Biophys. J. 99 (2010) 1397–1407.
[45] S. Ganguly, A.H.A. Clayton, A. Chattopadhyay, Organization of higher-order oligomers of the serotonin$_{1A}$ receptor explored utilizing homo-FRET in live cells, Biophys. J. 100 (2011) 361–368.
[46] R. Thomas, R. D'Ari, Biological Feedback, CRC Press, Boca Raton, Florida, 1990.
[47] R.P. Kulkarni, M. Bak-Maier, S.E. Fraser, Differences in protein mobility between pioneer versus follower growth cones, Proc. Natl Acad. Sci. U. S. A. 104 (2007) 1207–1212.
[48] M. Zaccolo, G.D. Benedetto, V. Lissandron, L. Mancuso, A. Terrin, I. Zamparo, Restricted diffusion of a freely diffusible second messenger: mechanisms underlying compartmentalized cAMP signaling, Biochem. Soc. Trans. 34 (2006) 495–497.
[49] H.J. Song, G.L. Ming, M.M. Poo, cAMP-induced switching in turning direction of nerve growth cones, Nature 388 (1997) 275–279.
[50] G.L. Ming, H.J. Song, B. Berninger, C.E. Holt, M. Tessier-Lavigne, M.M. Poo, cAMP-dependent growth cone guidance by netrin-1, Neuron 19 (1997) 1225–1235.
[51] A.B. Karlsson, E.T. Maizels, M.P. Flynn, J.C. Jones, E.A. Shelden, J.R. Bamburg, M. Hunzicker-Dunn, Luteinizing hormone receptor-stimulated progesterone production by preovulatory granulosa cells requires protein kinase A-dependent activation/dephosphorylation of the actin dynamizing protein cofilin, Mol. Endocrinol. 24 (2010) 1765–1781.